Chemical Bonding

International Edition: DOI: 10.1002/anie.201505665
German Edition: DOI: 10.1002/ange.201505665

Trimethylaluminum: Bonding by Charge and Current Topology

Hans-Georg Stammler, Sebastian Blomeyer, Raphael J. F. Berger, and Norbert W. Mitzel**

In memory of Evelyn Algernon Valentine Ebsworth

Abstract: *The charge density distribution of the trimethylaluminum dimer was determined by high-angle X-ray diffraction of a single crystal and quantum-chemical methods and analyzed using the quantum theory of atoms in molecules. The data can be interpreted as Al_2Me_6 being predominantly ionically bonded, with clear indications of topological asymmetry for the bridging Al–C bonds owing to delocalized multicenter bonding. This interpretation is supported by the calculated magnetic response currents. The data shed new light on the bonding situation in this basic organometallic molecule, which was previously described by contradicting interpretations of bonding.*

Trimethylaluminum is of widespread technological interest. It is used as a methylation agent and as a Lewis acid, finds applications as a co-catalyst and source for the olefin-polymerization co-catalyst methylalumoxane, and is important in many catalytic and technological processes.[1] Its existence was first reported in 1866.[2] Structure elucidation in these early days provided conflicting results. A crystal structure determined in 1953 ascertained the methyl-bridged nature of Al_2Me_6[3] as one of the first examples of a metal alkyl species containing both terminal and bridging methyl groups, a now more firmly established class of compounds.[4]

Whereas the trimethyl compounds of the aluminum congeners boron[5] and gallium[6] are aggregated much more weakly in the solid state and are monomers in the gas phase, dimeric Al_2Me_6 appears to be the sole form of occurrence in condensed phases. However, trimethylaluminum is in an equilibrium between the monomeric and dimeric species in the gas phase, and its gas-phase structure was established by electron diffraction.[7]

Crystal X-ray diffraction results led to a variety of bonding models for the $Al(\mu_2\text{-}CH_3)Al$ bridging methyl groups. Initial work favored hydrogen atoms in the bridging units,[8] whereas later reinvestigations of the same diffraction data suggested bridging behavior of the hydrogen atoms and a substantial distortion of the bridging methyl group from local C_{3v} symmetry (**1**; Scheme 1).[9] This repeatedly formulated idea of Al···HC bridging[10,11] found heavy objection,[12] and further experiments[13] favored a structure with pentacoordinate carbon atoms (**2**, **3**) and no bonding contribution of the C–H units. This hypothesis was confirmed by a ^{27}Al NQR study.[14]

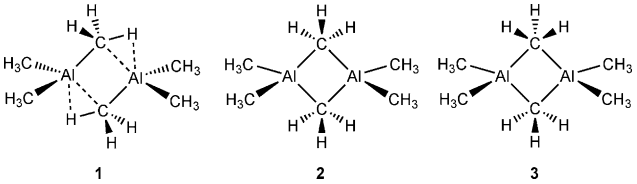

Scheme 1. Possible structures and bonding schemes of the dimer of trimethylaluminum, Al_2Me_6.

Powder neutron diffraction experiments on deuterated $Al_2(CD_3)_6$ at 4.5 K established the hydrogen positions in the sense of structure **3**.[15] Quantum-chemical calculations predicted molecular structure **2** (eclipsed bridging CH_3 groups, C_s symmetry) to be the lowest-energy conformer.[16] However, alternative structure **3** is only 0.3 kcal mol^{-1} higher in energy (staggered bridging CH_3 groups, C_{2h} symmetry). The barriers to rotation are very small so that at temperatures slightly higher than that of the neutron diffraction study, these hydrogen positions become dynamic,[17] as has been confirmed by NMR spectroscopy. These findings explain some of the earlier controversial debate.

Beside the various attempts in pinning down the structure, the interpretation of bonding remained controversial. Aside from the early considerations of C–H involvement, which can now with certainty be seen as invalid, multicenter bonding has been subject to debate. Haaland et al. reported an Al···Al distance of 2.619(5) Å for Al_2Me_6 and 2.617(6) Å for $Al_2Me_4H_2$ for the free molecules in the gas phase.[7] As these distances are only shorter than those in metallic aluminum by approximately 0.24 Å and only marginally surpass the sum of two covalent Al radii (2.50 Å),[18] these values seemed to support the view of direct bonding between the aluminum atoms in Al_2Me_6 and $Al_2Me_4H_2$.[19] In contrast, the Al···Al distances determined for the gaseous halide dimers Al_2Cl_6 (3.102(36) Å), Al_2Br_6 (3.288(78) Å), and Al_2I_6 (3.335(180) Å) are much longer and more than 0.25 Å longer than the Al···Al distance in the metal.[20]

[*] Dr. H.-G. Stammler, M. Sc. S. Blomeyer, Prof. Dr. N. W. Mitzel
Lehrstuhl für Anorganische Chemie und Strukturchemie
Centrum für Molekulare Materialien CM^2, Fakultät für Chemie
Universität Bielefeld
Universitätsstrasse 25, 33615 Bielefeld (Germany)
E-mail: mitzel@uni-bielefeld.de
Priv.-Doz. Dr. R. J. F. Berger[+]
Materialchemie, Paris-Lodron Universität Salzburg
Hellbrunner Strasse 34, 5020 Salzburg (Austria)
[+] Current address: Laboratory for Instructions in Swedish
University of Helsinki
A.I. Virtanens Plats 1, 00014 Helsinki (Finland)

Supporting information for this article is available on the WWW under http://dx.doi.org/10.1002/anie.201505665.

Contemporary textbooks of organometallic chemistry still speculate about hybridization of the aluminum atoms on the basis of structural data.[21] The common interpretation is that sp^3-hybridized Al and C(bridge) atoms form two 2-electron-3-center (2e3c) bonds (Scheme 2a). However, the large C-Al-C angle to the terminal methyl groups of 123° seems also to provide evidence for an sp^2-hybridized aluminum atom, which would require 2-electron-4-center (2e4c) bonding involving the two p orbitals at the aluminum atoms as well as two bridging methyl groups on one side and an Al–Al bond formed by an overlap of sp^2 hybrids on the other (Scheme 2b). Although a rather simplistic and extreme representation, this picture remains present in the thinking of generations of chemists and is still used in teaching.

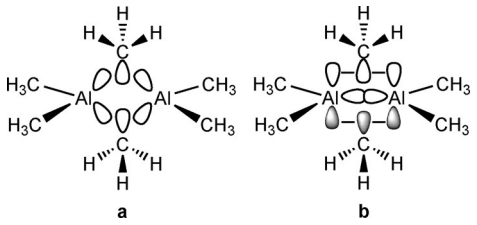

Scheme 2. Two possible pictures of the orbital interaction describing multicenter bonding in the dimer of trimethylaluminum, Al_2Me_6.

The charge-density distribution is expected to shed more light onto the bonding situation. However, it is known that the charge-density topologies of small ring systems can be complicated owing to the effects of two or more competing bonding components if one dominates the others.[22] The close proximity of more than two atoms in small rings makes the overlapping of such bonding components more likely.

Charge density is an observable quantity and experimentally available by high-angle X-ray diffraction. A crystal of Al_2Me_6 was grown for this purpose, and the diffraction experiment was carried out at 93 K up to diffraction angles of $2\theta = 101°$. The electron-density distribution was obtained using the Hansen–Coppens multipole formalism,[23] as implemented in the XD2006 program for multipole refinement.[24]

At 93 K, the earlier described methyl-group dynamics (solid-state NMR) are observable in the high-resolution experiment (Figure 1). It manifests itself in a 1:1 splitting of the hydrogen positions observed for one of the bridging and one of the terminal methyl groups, confirming the dynamics of the methyl group rotation that is populated here.[25] The mentioned powder neutron diffraction data at 4.5 K do not show these dynamics; at this temperature, the compound therefore seems to adopt its ground-state conformation.

The structural parameters of the new high-resolution X-ray diffraction experiment in comparison with the neutron powder diffraction data are listed in Table 1. Significant differences in the distances and angles are observed, which are beyond what one would expect to be due to a temperature difference of 90 K. However, the physical principles behind these measurements are different, and thus some deviation is to be expected.[26]

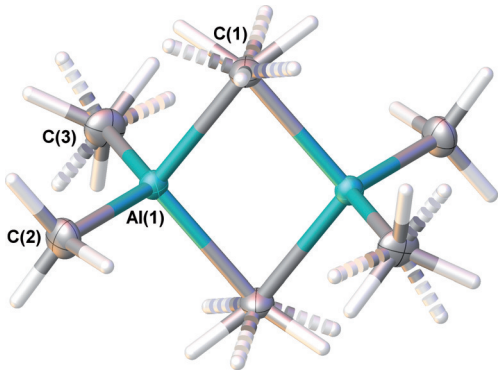

Figure 1. Structure of Al_2Me_6 as determined by X-ray diffraction at 93 K.

Table 1: Structural parameters of Al_2Me_6 as determined by X-ray diffraction at 93 K (XRD) after multipole refinement and those determined by neutron powder diffraction at 4.5 K (NPD) for comparison.[a][15]

Distance [Å]			Angle [°]		
	XRD	NPD		XRD	NPD
			—bridging—		
Al–C(1)	2.1205(2)	2.145(7)	Al-C(1)-Al′	75.49(1)	78.0(3)
Al–C(1)′	2.1252(2)	2.146(8)	C(1)-Al-C(1)′	104.52(1)	102.0(3)
			—terminal—		
Al–C(2)	1.9526(2)	1.945(6)	C(2)-Al-C(3)	123.55(1)	125.8(3)
Al–C(3)	1.9586(2)	1.926(5)	C(1)-Al-C(3)	107.26(1)	109.3(3)
Al···Al′	2.5988(1)	2.70(1)	C(1)-Al-C(2)	106.79(1)	103.3(3)
			C(1)′-Al-C(2)	107.26(1)	108.8(4)
			C(1)′-Al-C(3)	106.00(1)	105.3(3)

[a] Symmetry code: $^1/_2-x$, $^1/_2-y$, $1-z$.

Compared to the earlier structure determination by X-ray diffraction in 1970,[13] most parameters of this present work are the same within experimental error. Only parameters involving the C(3) carbon atom are slightly different: The Al–C(3) distance is slightly longer (1.9586(2) Å vs. 1.949(2) Å), and the C(1)′-Al-C(3) angle is smaller (106.00(1)° vs. 107.3(1)°).

The experimental electron-density distribution was analyzed along the lines of the quantum theory of atoms in molecules (QTAIM)[27] by the XD program.[24] The QTAIM parameters at bond critical points (bcps) are listed in Table 2. The typical, curved appearance of the atomic-interaction lines (AILs) in 2e3c bonds is superimposed onto the electron density in Figure 2. In this respect, it compares well with the graphs of diborane[28] and other boranes.[27]

However, there is a bond path between the two carbanionic ring members, topologically dividing the Al_2C_2 ring into two joined three-membered AlC_2 rings accompanied by two nearby AlCC ring critical points (rcps). This topological feature is reproduced by a quantum-chemically generated electron-density distribution (MP2/aug-cc-pVTZ).[29] This charge-density feature finds its counterpart in the topology of magnetically induced currents (see Figure 4 and explanation below). It is worth noting that the difference in the absolute electron density between the C–C bcp (exp. 0.177(2), calcd. 0.250 e Å^{-3}) and the two rcps (exp. 0.1765, calcd.

Table 2: QTAIM parameters for Al_2Me_6 for the asymmetric unit based on XRD data (exp) as well as quantum-chemical calculations (calcd).[a]

Bond	$\rho(r_{bcp})$		$\nabla^2\rho(r_{bcp})$		ε	
	exp	calcd	exp	calcd	exp	calcd
Al(1)–C(1)	0.323(3)	0.362	5.119(3)	4.719	0.33	0.28
Al(1)–C(1)′	0.276(3)	0.362	5.303(3)	4.719	0.38	0.28
Al(1)–C(2)	0.541(2)	0.579	7.684(3)	7.500	0.06	0.00
Al(1)–C(3)	0.531(2)	0.579	7.997(2)	7.500	0.05	0.00
C(1)–C(1)′	0.177(2)	0.250	0.230(1)	0.373	6.87	3.12
Bond (contd)	*d*(A–B)		*d*(A–bcp)		*d*(B–bcp)	
	exp	calcd	exp	calcd	exp	calcd
Al(1)–C(1)	2.1254	2.146	0.848	0.834	1.2769	1.312
Al(1)–C(1)′	2.1351	2.146	0.854	0.834	1.2806	1.312
Al(1)–C(2)	1.9528	1.952	0.795	0.778	1.1576	1.175
Al(1)–C(3)	1.9589	1.952	0.794	0.778	1.1647	1.175
C(1)–C(1)′	3.3614	3.366	1.6807	1.683	1.6807	1.683
Bond (contd)	λ_1		λ_2		λ_3	
	exp	calcd	exp	calcd	exp	calcd
Al(1)–C(1)	−1.78	−1.59	−1.34	−1.25	8.24	7.57
Al(1)–C(1)′	−1.60	−1.59	−1.16	−1.25	8.07	7.57
Al(1)–C(2)	−3.25	−2.79	−3.07	−2.74	14.0	13.0
Al(1)–C(3)	−3.25	−2.79	−1.34	−2.74	14.3	13.0
C(1)–C(1)′	−0.64	−0.79	−0.08	−0.19	0.96	1.35

[a] Electron density at the bond critical point (bcp) $\rho(r_{bcp})$ in $e\,Å^{-3}$, Laplacian at the bcp $\nabla^2\rho(r_{bcp})$ in $e\,Å^{-5}$, distance along the atomic interaction line between nuclei A and B (d(A–B)), distances between the bcp and the nuclei along the atomic interaction lines (d(A–bcp) and d(B–bcp); all distances in Å), Hessian eigenvalues (λ_1, λ_2, and λ_3) in $e\,Å^{-5}$, and ellipticity at the bcp (ε).

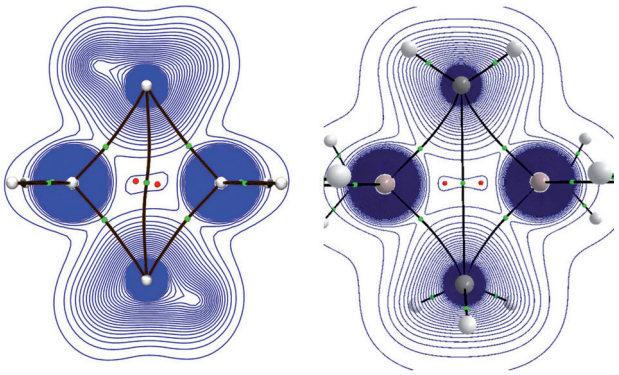

Figure 2. Experimentally determined (left) and calculated (right) electron-density distributions in the Al/Al′/C(1)/C(1)′ plane with superimposed atomic interaction lines and critical points.

0.245 $e\,Å^{-3}$) is very small, that is, the region in the middle of the Al_2C_2 ring is quite shallow in electron density. This almost merging of the ring and bond critical points is close to what is called a bond catastrophe and expresses a topologically unstable situation.[30] The fact that a bond path is observed between the two carbon atoms is reminiscent of the situation in electron-poor framework compounds, such as the intermetallic compound ZnSb.[31] In the present case of Al_2Me_6, this feature is likely to be the result of an overlap between the two carbanion basins of relatively high electron density, while the highly electron-deficient aluminum atoms contribute only a small amount of electron density to the central region of the ring. It is, however, their highly positive charge that attracts the carbanionic sites and positions them close enough to result in the described C–C bond path.

In comparison with the terminal Al–C bonds, the bridging Al–C bonds in Al_2Me_6 are approximately 0.17 Å longer. They are also of significantly lower electron density at the bcps (0.28–0.36 $e\,Å^{-3}$) than the terminal bonds (0.53–0.58 $e\,Å^{-3}$). A similar situation has been observed for $Y(AlEt_4)_3$ concerning the Y,Al bridging and terminal Al–C bonds.[32] These low values and the moderately positive Laplacian values at the bcps $\nabla^2\rho(r_{bcp})$ (Figure 3) are indicative of closed-shell-type

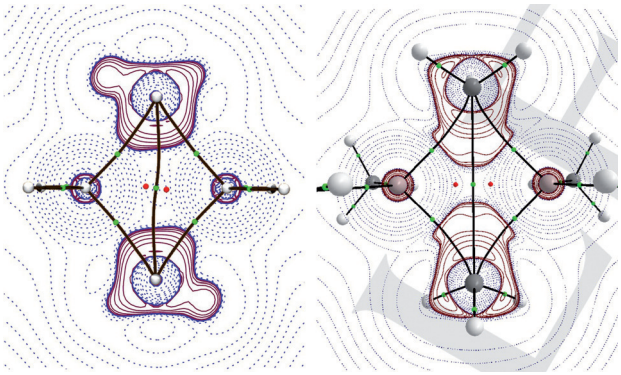

Figure 3. Laplacian plots of the experimentally determined (left) and calculated (right) electron-density distributions in the Al/Al′/C(1)/C(1)′ plane. Dotted lines denote positive, solid lines negative values.

interactions between the Al and C atoms, that is, a strongly ionic nature of these bonds. However, both kinetic ($G(r_{bcp})$ = 0.407 Hartree $Å^{-3}$) and potential-energy densities ($V(r_{bcp})$ = −0.483 Hartree $Å^{-3}$) at the bcps and the resulting slightly negative local energy density $H(r_{bcp}) = -0.076$ Hartree $Å^{-3}$ suggest some partially covalent character for the Al–C_b bonds (MP2).[33]

An interesting detail of the bonding situation is the very different bond ellipticity of the bridging and terminal Al–C bonds. Whereas the terminal bonds behave as expected and show ellipticity values of 0.05 and 0.06, that is, close to zero as expected for a σ-type bond, the bridging bond paths have ellipticity values of 0.33 and 0.38. This asymmetry along the bond paths is due to the involvement of more than two nuclear attractors in bonding and is thus indicative of polar multicenter bonding.

Ring and cage topologies often annihilate bond paths, yielding ring- or cage-critical points. Moreover, extremely elongated bonds are not necessarily connected with an accumulation of electron density at the center of the bond.[34] Therefore, we were interested in alternative properties to characterize the nature of the bonding in Al_2Me_6 that do not suffer from such deficits. A homopolar covalent Al–Al bond in the center of the molecule is expected to cause a significant diamagnetic response in a homogeneous magnetic field perpendicular to this bond. This is a consequence of the magnetic invocation of a virtual transition between an occupied σ and a corresponding unoccupied σ* orbital.[35] Such a diamagnetic response is stronger for smaller energy

gaps. Ethane, for example, sustains a magnetically induced ring current of approximately 8 nAT^{-1} around its center of symmetry.

For an elongated Al–Al bond, the energy gap is expected to be smaller than that of a C–C single bond, hence the expected currents should be larger for Al_2Me_6 with a substantial Al–Al bond than for ethane. Related bonding situations have been examined in low-valent silicon clusters with elongated central Si–Si 2e2c bonds.[37] In these cases, diatropic total molecular ring currents of 10–12 nAT^{-1} have been observed. For Al_2Me_6, we have now calculated[38] a diatropic total molecular current of 1.5 nAT^{-1}. On the basis of this magnetic criterion, we again rule out the hypothesis of a central Al–Al bond in Al_2Me_6. Inspection of a streamline plot of the induced current density field (Figure 4) shows two diatropic vortices, close to the bridging

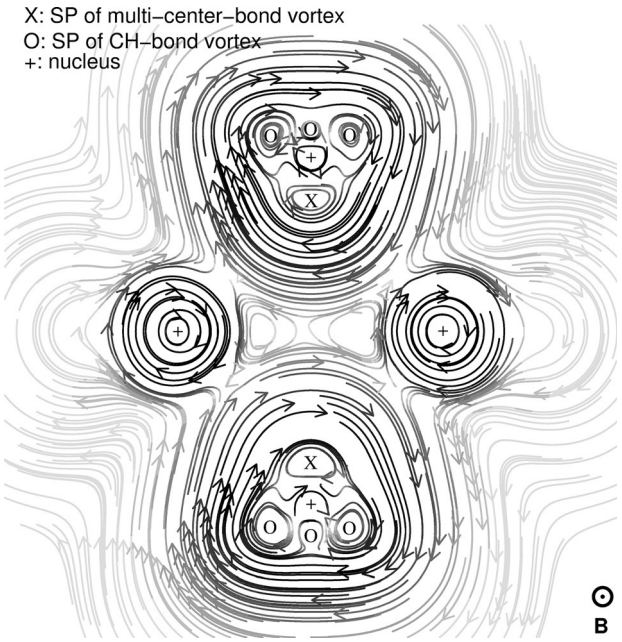

Figure 4. Streamline plot of the magnetically induced current densities[36] in Al_2Me_6 in the Al/Al′/C(1)/C(1)′ plane. The external homogenous magnetic field is pointing out of the plane; hence domains with local para/diamagnetic response show a counterclockwise/clockwise curl (para/diatropic).

carbon atoms, which neither originate from C–H bonds nor are atom-centered. Hence, we conclude these two vortices (stagnation points[39] (SP) in Figure 4) to be current signatures of 2e3c bonds (Al–C–Al). This is in agreement with the above AIM analysis and finds its direct resemblance in the local charge-density concentration visible in the Laplacian plots of the experimental and calculated electron densities (Figure 3) in this region of the molecule. The two current vortices along the Al···Al line (Figure 4) are paralleled by the occurrence of two rcps and a bond path in the QTAIM picture between the two bridging carbon atoms for the calculated density (Figure 3). This finding hints again (as previously suggested)[40] at the so far unexplored, but very likely close analytical relation between the topology of the electron density and the topology of the magnetically induced ring currents.

The idea of using structural parameters, for example, the wide angle C_{term}-Al-C_{term} to deduce a hybridization state could have been already objected on the basis of VSEPR[41] considerations; they now find an upgraded foundation in the electron density and current picture. The two bridging Al–C bonds with their much lower electron densities than the terminal ones require less space in the coordination sphere of the aluminum atom (Figure 1). It follows that compared to an ideal tetrahedral coordination sphere, there will be a smaller C-Al-C angle for the bridging bonds (104.52(1)°) and a larger C-Al-C angle for the terminal bonds (123.55(1)°).

Our present electron-density investigation has led to a clear picture of the nature of bonding in Al_2Me_6 as a molecule with multicenter bonds of very ionic nature. This bonding model is in agreement with the calculated magnetic response current density field. This shows current vortices close to the bridging CH_3 groups assignable to two 2e3c bonds and two current vortices along the Al···Al line that are related to the occurrence of a bond path in the QTAIM picture between the two bridging carbon atoms. Care should be taken not to over-interpret this C–C bond path in the sense of an ethane molecule with two electron-deficient $AlMe_2$ units participating in the electron density of a weak C–C bond. The existence of this feature is likely due to the dominance of the high contribution of the carbanionic units to electron density in the ring in the presence of electron-poor aluminum atoms. The integrated total molecular current (susceptibility) of 1.5 nAT^{-1} is much smaller than expected for a molecule with a central electron-delocalized Al–Al bond but agrees well with what is expected for an ionic aggregate.

Acknowledgements

This work was supported by the Deutsche Forschungsgemeinschaft (core facility GED@BI, Mi477/21-1) and the Magnus Ehrnrooth Foundation. We thank Dr. Yuriy V. Vishnevskiy for help with data analyses with AIMALL and Dr. Benedikt Waerder for the preparation of the capillaries with Al_2Me_6.

Keywords: aluminum · chemical bonding · electron density · ring currents · topology · X-ray diffraction

How to cite: *Angew. Chem. Int. Ed.* **2015**, *54*, 13816–13820
Angew. Chem. **2015**, *127*, 14021–14026

[1] a) *Chemistry of Aluminium, Gallium, Indium and Thallium* (Ed.: A. J. Downs), Chapman and Hall, London, **1993**; b) M. Brookhart, M. L. H. Green, L.-L. Wong, *Prog. Inorg. Chem.* **1988**, *36*, 1; c) F. Ghiotto, C. Pateraki, J. Tanskanen, J. R. Severn, N. Luehmann, A. Kusmin, J. Stellbrink, M. Linnolahti, M. Bochmann, *Organometallics* **2013**, *32*, 3354–3362.
[2] G. B. Buckton, W. Odling, *Liebigs Ann. Suppl.* **1866**, *4*, 110.
[3] P. H. Lewis, R. E. Rundle, *J. Chem. Phys.* **1953**, *21*, 986.
[4] a) A. Venugopal, I. Kamps, D. Bojer, R. J. F. Berger, A. Mix, A. Willner, B. Neumann, H.-G. Stammler, N. W. Mitzel, *Dalton Trans.* **2009**, 5755; b) D. Bojer, A. Venugopal, B. Neumann, H.-

G. Stammler, N. W. Mitzel, *Angew. Chem. Int. Ed.* **2010**, *49*, 2611; *Angew. Chem.* **2010**, *122*, 2665; c) M. Zimmermann, R. Anwander, *Chem. Rev.* **2010**, *110*, 6194; d) D. Bojer, A. Venugopal, A. Mix, B. Neumann, H.-G. Stammler, N. W. Mitzel, *Chem. Eur. J.* **2011**, *17*, 6248; e) D. Bojer, B. Neumann, H.-G. Stammler, N. W. Mitzel, *Chem. Eur. J.* **2011**, *17*, 6239; f) G. Occhipinti, C. Meermann, H. M. Dietrich, R. Litlabø, F. Auras, K. W. Törnroos, C. Maichle-Mössmer, V. R. Jensen, R. Anwander, *J. Am. Chem. Soc.* **2011**, *133*, 6323; g) A. Nieland, A. Mix, B. Neumann, H.-G. Stammler, N. W. Mitzel, *Eur. J. Inorg. Chem.* **2014**, 51.

[5] R. Boese, A. J. Downs, T. M. Greene, A. W. Hall, C. A. Morrison, S. Parsons, *Organometallics* **2003**, *22*, 2450 – 2457.

[6] a) N. W. Mitzel, C. Lustig, R. J. F. Berger, N. Runeberg, *Angew. Chem. Int. Ed.* **2002**, *41*, 2519 – 2522; *Angew. Chem.* **2002**, *114*, 2629 – 2632; b) N. W. Mitzel, C. Lustig, *Z. Naturforsch. B* **2004**, *59*, 140 – 147.

[7] A. Almenningen, S. Halvorsen, A. Haaland, *Acta Chem. Scand.* **1971**, *25*, 1937.

[8] R. G. Vranka, E. L. Amma, *J. Am. Chem. Soc.* **1967**, *89*, 3121.

[9] S. K. Byram, J. K. Fawcett, S. C. Nyburg, R. J. O′Brien, *J. Chem. Soc. Chem. Commun.* **1970**, 16.

[10] A. Burawoy, *Nature* **1945**, *155*, 269.

[11] K. S. Pitzer, H. S. Gutowsky, *J. Am. Chem. Soc.* **1946**, *68*, 2204 – 2209.

[12] F. A. Cotton, *Inorg. Chem.* **1970**, *9*, 2804.

[13] J. C. Huffmann, W. E. Streib, *J. Chem. Soc. D* **1971**, 911.

[14] M. J. S. Dewar, D. B. Patterson, *J. Chem. Soc. D* **1970**, 544.

[15] G. S. McGrady, J. F. C. Turner, R. M. Ibberson, M. Prager, *Organometallics* **2000**, *19*, 4398 – 4401.

[16] a) Y. S. Hiraoka, M. Mashita, *J. Cryst. Growth* **1994**, *145*, 473; b) G. Y. Hong, X. Y. Cao, D. X. Wang, L. M. Li, G. X. Xu, *Chin. J. Chem.* **1998**, *16*, 209; c) D. Berthomieu, Y. Bacquet, L. Pedocchi, A. Goursot, *J. Phys. Chem. A* **1998**, *102*, 7821.

[17] S. Albert, J. A. Ripmeester, *J. Chem. Phys.* **1979**, *70*, 722 – 725.

[18] *Table of Interatomic Distances and Configuration in Molecules and Ions* (Ed.: L. E. Sutton), The Chemical Society, London, **1958**.

[19] J. Emsley, *The Elements*, Clarendon Press, Oxford, **1991**.

[20] K. Aarset, Q. Shen, H. Thomassen, A. D. Richardson, K. Hedberg, *J. Phys. Chem. A* **1999**, *103*, 1644 – 1652.

[21] a) C. Elschenbroich, *Organometallchemie*, 6. Aufl., Teubner, Wiesbaden, **2008**; b) J. House, *Inorganic Chemistry*, Academic Press (Elsevier), Waltham, **2012**, p. 383; c) K.-Y. Akiba, *Organic Main Group Chemistry*, Wiley, Hoboken, **2011**, p. 82.

[22] a) N. W. Mitzel, U. Losehand, A. Wu, D. Cremer, D. W. H. Rankin, *J. Am. Chem. Soc.* **2000**, *122*, 4471 – 4482; b) N. W. Mitzel, K. Vojinović, R. Fröhlich, T. Foerster, D. W. H. Rankin, *J. Am. Chem. Soc.* **2005**, *127*, 13705 – 13713; c) W. Scherer, G. Eickerling, D. Shorokhov, E. Gullo, G. S. McGradyc, P. Sirsch, *New J. Chem.* **2006**, *30*, 309 – 312; d) W. Scherer, V. Herz, A. Brück, C. Hauf, F. Reiner, S. Altmannshofer, D. Leusser, D. Stalke, *Angew. Chem. Int. Ed.* **2011**, *50*, 2845 – 2849; *Angew. Chem.* **2011**, *123*, 2897 – 2902; e) D. Winkelhaus, Y. V. Vishnevskiy, R. J. F. Berger, H.-G. Stammler, B. Neumann, N. W. Mitzel, *Z. Anorg. Allg. Chem.* **2013**, *639*, 2086 – 2095.

[23] N. K. Hansen, P. Coppens, *Acta Crystallogr. Sect. A* **1978**, *34*, 909 – 921.

[24] XD2006—A Computer Program Package for Multipole Refinement, Topological Analysis of Charge Densities and Evaluation of Intermolecular Energies from Experimental and Theoretical Structure Factors, A. Volkov, P. Macchi, L. J. Farrugia, C. Gatti, P. Mallinson, T. Richter, T. Koritsanszky, **2006**.

[25] Using *SHELX*-97 (G. M. Sheldrick, *Acta Crystallogr. Sect. A* **2008**, *64*, 112 – 122) with a reflection subset up to a resolution of 0.81 Å, the positions of all hydrogen atoms were located in a difference Fourier transformation and refined with free site occupation factors. The resulting occupations were not significantly different from 0.5, so this value was fixed. The positions were also refined in XD2006, but the C–H distances were restrained to 1.083 Å. The *U*(iso) values of the hydrogen atoms were constrained to be equal to 1.5 times the *U*(eq) value of the attached carbon atoms.

[26] D. W. H. Rankin, N. W. Mitzel, C. A. Morrison, *Structural Methods in Molecular Inorganic Chemistry*, 1st ed., Wiley, Chichester, **2013**.

[27] a) R. F. W. Bader, *Atoms in Molecules: A Quantum Theory*, Clarendon Press, Oxford, **1990**; b) P. L. A. Popelier, *Atoms in Molecules - An Introduction*, Prentice Hall, **2000**; c) C. F. Matta, R. J. Boyd, *The Quantum Theory of Atoms in Molecules*, Wiley-VCH, Weinheim, **2007**.

[28] R. F. W. Bader, S. G. Anderson, A. J. Duke, *J. Am. Chem. Soc.* **1979**, *101*, 1389 – 1395.

[29] For details of the calculations, see the Supporting Information.

[30] a) L. J. Farrugia, C. Evans, D. Lentz, M. Roemer, *J. Am. Chem. Soc.* **2009**, *131*, 1251 – 1268; b) L. J. Farrugia, H. M. Senn, *J. Phys. Chem. A* **2010**, *114*, 13418 – 13433; c) J. Henn, D. Leusser, D. Stalke, *J. Comput. Chem.* **2007**, *28*, 2317 – 2324; d) H. Jacobsen, *J. Comput. Chem.* **2009**, *30*, 1093 – 1102.

[31] A. Fischer, E.-W. Scheidt, W. Scherer, D. E. Benson, Y. Wu, D. Eklöf, U. Häussermann, *Phys. Rev. B* **2015**, *91*, 224309.

[32] M. G. Klimpel, R. Anwander, M. Tafipolsky, W. Scherer, *Organometallics* **2001**, *20*, 3983 – 3992.

[33] a) D. Cremer, E. Kraka, *Croat. Chem. Acta* **1984**, *56*, 1259 – 1281; b) D. Cremer, E. Kraka, *Angew. Chem. Int. Ed. Engl.* **1984**, *23*, 627 – 628; *Angew. Chem.* **1984**, *96*, 612 – 614.

[34] D. Nied, R. Köppe, W. Klopper, H. Schnöckel, F. Breher, *J. Am. Chem. Soc.* **2010**, *132*, 10264 – 10265.

[35] a) E. Steiner, P. W. Fowler, *J. Phys. Chem. A* **2001**, *105*, 9553; b) E. Steiner, P. W. Fowler, *Chem. Commun.* **2001**, 2220; c) P. W. Fowler, E. Steiner, L. W. Jenneskens, *Chem. Phys. Lett.* **2003**, *371*, 719.

[36] For practical reasons, we use the terms “currents” or “induced currents” in the following for what should most specifically be called “magnetically induced electronic probability current susceptibility density vector field”.

[37] a) R. J. F. Berger, H. S. Rzepa, D. Scheschkewitz, *Angew. Chem. Int. Ed.* **2010**, *49*, 10006; *Angew. Chem.* **2010**, *122*, 10203; b) K. Abersfelder, A. J. P. White, R. J. F. Berger, H. S. Rzepa, D. Scheschkewitz, *Angew. Chem. Int. Ed.* **2011**, *50*, 7936; *Angew. Chem.* **2011**, *123*, 8082; c) A. Jana, V. Huch, M. Repisky, R. J. F. Berger, D. Scheschkewitz, *Angew. Chem. Int. Ed.* **2014**, *53*, 3514; *Angew. Chem.* **2014**, *126*, 3583; d) D. Kratzert, D. Leusser, J. J. Holstein, B. Dittrich, K. Abersfelder, D. Scheschkewitz, D. Stalke, *Angew. Chem. Int. Ed.* **2013**, *52*, 4478 – 4482; *Angew. Chem.* **2013**, *125*, 4574 – 4578.

[38] For DFT-based magnetic response calculations using London orbitals as implemented in the GIMIC program, see: a) J. Jusélius, D. Sundholm, J. Gauss, *J. Chem. Phys.* **2004**, *121*, 3952; b) H. Fliegl, S. Taubert, O. Lehtonen, D. Sundholm, *Phys. Chem. Chem. Phys.* **2011**, *13*, 20500; for details, see the Supporting Information.

[39] Because of current conservation, the points in space with no current, so-called stagnation points (SPs), can be used for a unique topological description of the current field.

[40] J. E. Barquera-Lozada, A. Obenhuber, C. Hauf, W. Scherer, *J. Phys. Chem. A* **2013**, *117*, 4304 – 4315.

[41] R. J. Gillespie, P. A. Popelier, *Chemical Bonding and Molecular Geometries—From Lewis to Electron Densities*, Oxford University Press, New York, **2001**.

Received: June 19, 2015
Revised: August 10, 2015
Published online: September 22, 2015

